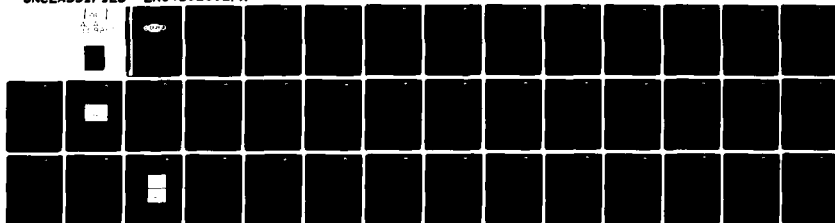


AD-A109 817 ROCKWELL INTERNATIONAL THOUSAND OAKS CA MICROELECTR--ETC F/G 20/3
RESEARCH IN MULTI-COLOR THIN FILM EMITTERS.(U)
DEC 81 L G HALE N00014-79-C-0341
UNCLASSIFIED ERC41026.2FR ML



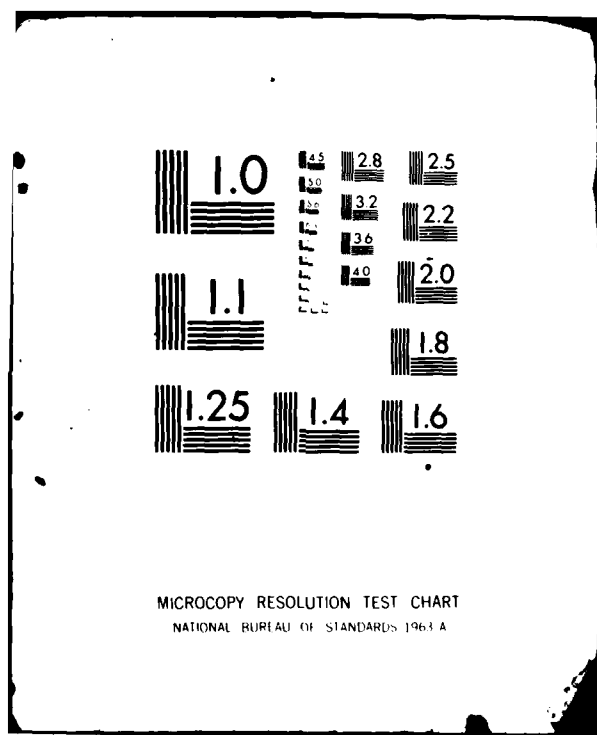
END

DATE

FILMED

82

DTIC



AD A109817

LEVEL IV

12

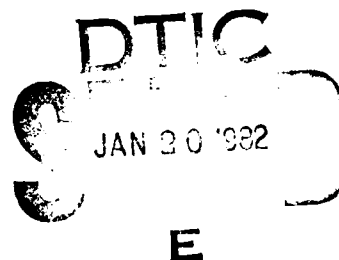
14



RESEARCH IN MULTI-COLOR THIN FILM EMITTERS

L. HALE

ROCKWELL INTERNATIONAL SCIENCE CENTER
THOUSAND OAKS
CALIFORNIA
91360



CONTRACT N00014-79-C-0341

DECEMBER 1981

FINAL REPORT FOR PERIOD 15 MARCH 79 - 30 SEPT 81

Approved for public release; distribution unlimited



PREPARED FOR THE
OFFICE OF NAVAL RESEARCH • 800 N. QUINCY ST. • ARLINGTON, VA. 22217

01 19 82 092

DTIC FILE COPY

UNCLASSIFIED

SECURITY CLASSIFICATION OF THIS PAGE (When Data Entered)

| REPORT DOCUMENTATION PAGE | | READ INSTRUCTIONS BEFORE COMPLETING FORM |
|--|-------------------------------------|--|
| 1. REPORT NUMBER | 2. GOVT ACCESSION NO. 4D-1109817 | 3. RECIPIENT'S CATALOG NUMBER |
| 4. TITLE (and Subtitle) RESEARCH IN MULTI-COLOR THIN FILM EMITTERS | | 5. TYPE OF REPORT & PERIOD COVERED Final Report for the Period 03/15/79 - 09/30/81 |
| | | 6. PERFORMING ORG. REPORT NUMBER ERC41026.2FR |
| 7. AUTHOR(s) L. G. Hale | | 8. CONTRACT OR GRANT NUMBER(s) N00014-79-C-0341 |
| 9. PERFORMING ORGANIZATION NAME AND ADDRESS Microelectronics Research & Development Center Rockwell International Corporation Thousand Oaks, CA 91360 | | 10. PROGRAM ELEMENT, PROJECT, TASK AREA & WORK UNIT NUMBERS |
| 11. CONTROLLING OFFICE NAME AND ADDRESS Scientific Officer, Office of Naval Research 800 North Quincy Street Arlington, VA 22217 | | 12. REPORT DATE December, 1981 |
| | | 13. NUMBER OF PAGES 39 |
| 14. MONITORING AGENCY NAME & ADDRESS (if different from Controlling Office) | | 15. SECURITY CLASS. (of this report) Unclassified |
| | | 15a. DECLASSIFICATION/DOWNGRADING SCHEDULE |
| 16. DISTRIBUTION STATEMENT (of this Report) Approved for public release; distribution unlimited | | |
| 17. DISTRIBUTION STATEMENT (of the abstract entered in Block 20, if different from Report) | | |
| 18. SUPPLEMENTARY NOTES | | |
| 19. KEY WORDS (Continue on reverse side if necessary and identify by block number) Electroluminescence Thin Film Color emitter | | |
| 20. ABSTRACT (Continue on reverse side if necessary and identify by block number) A green thin film electroluminescent emitter has been developed capable of greater than 700 fL brightness. This is the brightest green EL device reported to date. In addition, both a blue and a red thin film emitter have been fabricated. The red emitter produced 15 fL and the blue 1 fL. The device is a multilayer structure consisting of a rare earth activated ZnS layer sandwiched between two dielectric layers of Y ₂ O ₃ . | | |

412310

DD FORM 1 JAN 73 1473

EDITION OF 1 NOV 65 IS OBSOLETE

UNCLASSIFIED

SECURITY CLASSIFICATION OF THIS PAGE (When Data Entered)



TABLE OF CONTENTS

| | <u>Page</u> |
|-------------------------------------|-------------|
| 1.0 SUMMARY..... | 1 |
| 2.0 BACKGROUND..... | 2 |
| 3.0 MATERIALS FABRICATION..... | 4 |
| 4.0 ELECTRO-OPTIC MEASUREMENTS..... | 6 |
| 5.0 CONCLUSION..... | 33 |
| 6.0 REFERENCES..... | 35 |

| | |
|---------------|---|
| Accession For | |
| NTIS REARI | X |
| DTIC TAB | |
| Unannounced | |
| Justification | |
| By _____ | |
| Distribution | |
| Availability | |
| Dist | |
| A | |



LIST OF FIGURES

| | <u>Page</u> |
|---|-------------|
| Fig. 1 Thin film EL structure..... | 5 |
| Fig. 2 Room temperature spectrum of an annealed ZnS:SmF ₃ thin film emitter..... | 7 |
| Fig. 3 Room temperature spectrum of an unannealed ZnS:SmF ₃ thin film emitter..... | 8 |
| Fig. 4 Decay time of ZnS:SmF ₃ film (a) upper trace; voltage pulse, (b) lower trace; light output..... | 10 |
| Fig. 5 Room temperature spectrum of ZnS:Sm ₂ S ₃ thin film emitter..... | 12 |
| Fig. 6 Decay curve for ZnS:SmF ₃ showing double slope..... | 13 |
| Fig. 7 Auger depth profile of ZnS:Sm ₂ S ₃ thin film emitter..... | 14 |
| Fig. 8 Room temperature spectrum of ZnS:EuF ₃ thin film emitter..... | 15 |
| Fig. 9 Room temperature spectrum of ZnS:TmF ₃ thin film emitter..... | 17 |
| Fig. 10 Photopic response human eye..... | 18 |
| Fig. 11 Room temperature spectrum of ZnS:TbF ₃ thin film emitter..... | 19 |
| Fig. 12. Ratio of $^5D_3 \rightarrow ^7F_4$ / $^5D_4 \rightarrow ^7F_6$) transitions vs applied field for ZnS:TbF ₃ film..... | 21 |
| Fig. 13 Brightness vs voltage results of this program compared to published reports..... | 22 |
| Fig. 14 Electronic current vs (field across ZnS) ⁻¹ for ZnS:TbF ₃ thin film..... | 24 |
| Fig. 15 Technique for separating electronic current from displacement current..... | 25 |
| Fig. 16 Decay curve for ZnS:TbF ₃ thin film showing double slope..... | 27 |
| Fig. 17 (a), (b), (c), (d). Effect of annealing ZnS:TbF ₃ thin film emitter at constant temperature for different times..... | 28 |
| Fig. 18 Brightness vs voltage curve for ZnS:SmF ₃ thin film emitter..... | 30 |
| Fig. 19 Brightness vs voltage curve for ZnS:TmF ₃ thin film emitter..... | 31 |



1.0 SUMMARY

The objective of this program was to evaluate the feasibility of incorporating rare earth fluorides into a thin film ZnS matrix in order to fabricate a multi-color electroluminescent display. The rare-earths were chosen because their spectra covers the visible region and they are in general narrow band emitters. In addition, it has been found with color phosphors for television, that narrow band emitters provided the best luminous efficiency (i.e., the ratio of the emitted luminous flux to the power supplied).¹ Luminous flux is that part of the radiated energy to which the eye is sensitive. The rare-earth fluorides of terbium, samarium, europium and thulium were investigated during the period of this program. Described in this report are the results of characterizing these thin film emitters. The characterization includes: 1) optical spectrum; 2) brightness-voltage-efficiency curves; 3) decay time measurements; 4) annealing experiments; and 5) depth profiling measurements by Auger spectroscopy.

In summary, the results show that a green emitting thin film electroluminescent device capable of producing a brightness of 700 fL was observed. This is the first time such a high brightness green emitting device has been reported.² In addition, a cursory investigation has produced a red emitting thin film (ZnS:SmF₃) capable of 15 fL and a blue emitting thin film capable of <1 fL were also fabricated. The results for the red and blue emitters are far from optimized. These thin film electroluminescent emitters exhibit many of the characteristics required for a flat panel TV matrix display for military applications (e.g., immunity to ambient extremes of light, shock, vibration temperature nonlinear electro-optic response for matrix address, adequate time response to pulse excitation and low power consumption).



2.0 BACKGROUND

The objective of this program is to investigate multi-color thin film electroluminescent emitters using various rare-earth activators. The goal of the first phase of the program involved evaluating TbF_3 as an activator in a ZnS matrix to create a green emitting thin film emitter. In the final phase of the program, the rare-earth activators EuF_3 , SmF_3 and Sm_2S_3 were investigated to produce a red emitter.

The most efficient thin film phosphor system reported to date is manganese activated zinc sulfide (5 l/w).³ The Mn^{+2} ion is incorporated substitutionally for Zn^{+2} ion in the zinc sulfide lattice. Concentrations of 1-2% Mn give optimal performance. Luminescence is caused by impact excitation of the Mn^{+2} ion. The resultant emission spectrum is relatively broadband peaked at 5800Å (yellow) and also includes a weaker green and red component. The emission spectrum of Mn^{+2} is due to states internal to the manganese ion and therefore makes it less affected by the external ambient (temperature, electric field strength or frequency of excitation, host lattice impurities).

The atoms of the rare-earth metals differ from those of the other elements in that not only the outer electron shell but also a deeper shell is incompletely filled. Electronic transitions in this inner shell, caused by absorption or emission of radiation, are little disturbed by the environment, they are screened by the outer-most electrons. One result of this is that the spectral emission lines of the trivalent ions are very narrow. In this respect substances activated with trivalent rare-earths differ considerably from most other fluorescent substances whose fluorescence spectrum usually consists of broadband emission. Recent work on phosphors for CRT and fluorescent lamps using rare-earths has produced significant improvements in efficiency.⁴

The approach taken under this program utilized fabrication techniques developed at this laboratory which has yielded high brightness long-life thin film emitters using Mn activated ZnS. These films have the highest efficiency



ERC41026.2FR

reported to date (5 l/w). These fabrication techniques have allowed us to fabricate ZnS films activated with TbF_3 , which have a brightness of greater than 700 fL and efficiencies of 0.2 l/w. These are the brightest thin film electroluminescent devices using an activator other than manganese reported to date.²

Initially, samarium fluoride and europium fluoride were chosen for the red emission. Thulium fluoride was selected for the blue emission. It has been reported that incorporating the rare-earths as molecules of rare-earth fluorides increases the stability of the light emission of the films.⁵ In the molecular form, the fluorines act as charge compensation for the rare-earth ion. The europium ion can be either Eu^{+2} or Eu^{+3} . In the Eu^{+2} state, the emission is broadband with the dominant peak in the blue region of the spectrum. The emission of the Eu^{+3} consists of several lines with the main transition in the red (6100Å). The intensity of these transitions are determined by the crystal field of the host lattice. The dominant transition of the samarium ion is at 6490Å (red). This material has produced the brightest red emitter. As mentioned previously, the emission of the rare-earths is relatively independent of temperature and excitation frequency compared to other activators. This is an important consideration for a matrix addressed display operating over a wide temperature range since many frequency components are present in the matrix addressed system.



3.0 MATERIALS FABRICATION

The rare-earth activated ZnS films are made using the same fabrication techniques as used to make the high brightness, high efficiency Mn activated films. This consists of a "hot-wall" electron beam evaporation system which is microprocessor controlled. The activator is introduced by co-evaporation which is done in a resistance-heated boat. The thickness of the film is monitored with a laser monitor during deposition. The substrate is maintained at an elevated temperature through the use of quartz lamps in the vacuum chamber.

The films are fabricated on Corning glass 7059 coated with indium tin oxide. The structure which is shown in Fig. 1 consists of a transparent conductor, a layer of Y_2O_3 followed by a layer of ZnS doped with the appropriate activator, a second layer of Y_2O_3 followed by a conductor such as aluminum.

It has been found that in order to obtain optimum electroluminescence with the Mn film, it is necessary to anneal the films at an elevated temperature for about an hour. Films which are not annealed have a very low light output. This anneal procedure causes the manganese to redistribute to the proper site. Also the annealing improves the crystallization of ZnS.⁶ This procedure has been optimized for Mn activated emitters as evidenced by the highest efficiency reported to date.³

Preliminary results with the Tb activator indicate that the unannealed films are capable of emitting over 300 fL while the annealed samples were capable of emitting over 700 fL.

ERC41026.2FR

ERC80-9479

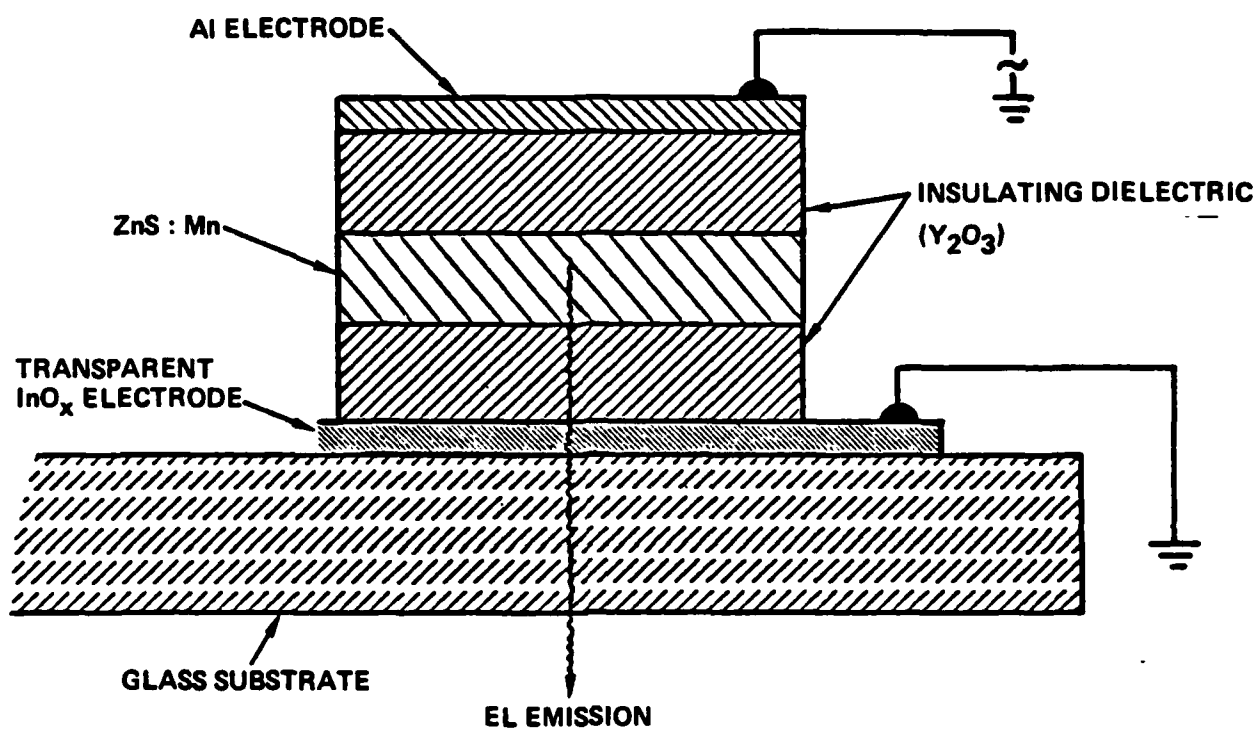


Fig. 1 Thin film EL structure.



ERC41026.2FR

4.0 ELECTRO-OPTIC MEASUREMENTS

Several electro-optic measurements were made on the thin film emitters: 1) the emission spectrum is made using a Jarrel Ash 0.5 meter monochromator and a PAR lock-in amplifier; 2) the brightness-voltage and the luminous conversion efficiency are measured using an HP 3052A data acquisition system. The activator concentration is determined using energy dispersive x-ray analysis (EDAX). In addition, concentration and depth profiles of some samples were determined using Auger electron spectroscopy (AES). Instantaneous decay time constants were determined from oscilloscope traces.

The room temperature spectra were recorded using a GaAs photomultiplier as the detector because of its flat spectral response across the visible spectrum. Figure 2 shows the room temperature spectrum of a ZnS:SmF₃ thin film EL emitter. It has the characteristic spectrum associated with the Sm⁺³ ion.⁷ Figure 3 shows the same sample before annealing. Previous work at this laboratory has shown that annealing tends to make the film more crystalline. The effect of annealing had only a slight change on the spectrum. Before annealing the higher energy transition $^4G_{5/2} \rightarrow ^6H_{5/2}$ (5650Å) does not appear to split while the lower energy transition $^4G_{5/2} \rightarrow ^6H_{9/2}$ (6490Å) has an additional level at 6810Å.

The crystal field establishes in part the oscillator strengths of the $4f^5$ transitions. With the free ion, all the $4f^5$ transitions have the same parity therefore, only the magnetic dipole and quadrupole transitions can occur. In this case, electric dipole transitions are forbidden. When the symmetry of the crystal field lacks a center of inversion electric dipoles are allowed. The transitions observed with the SmF₃ films are $^4G_{5/2} \rightarrow ^6H_{5/2}$ (5650Å), $^4G_{5/2} \rightarrow ^6H_{7/2}$ (6100Å) both magnetic dipole transitions ($\Delta J = 0, 1$, respectively) and $^4G_{5/2} \rightarrow ^6H_{9/2}$ (6490Å) an electric dipole transition ($\Delta J = 2$). When the Sm⁺³ is located at a center of inversion the electric dipole ($^4G_{5/2} \rightarrow ^6H_{9/2}$) transition should decrease and the magnetic dipole increase. When the ratio of the electric to the magnetic dipole transition is



ERC41026.2FR

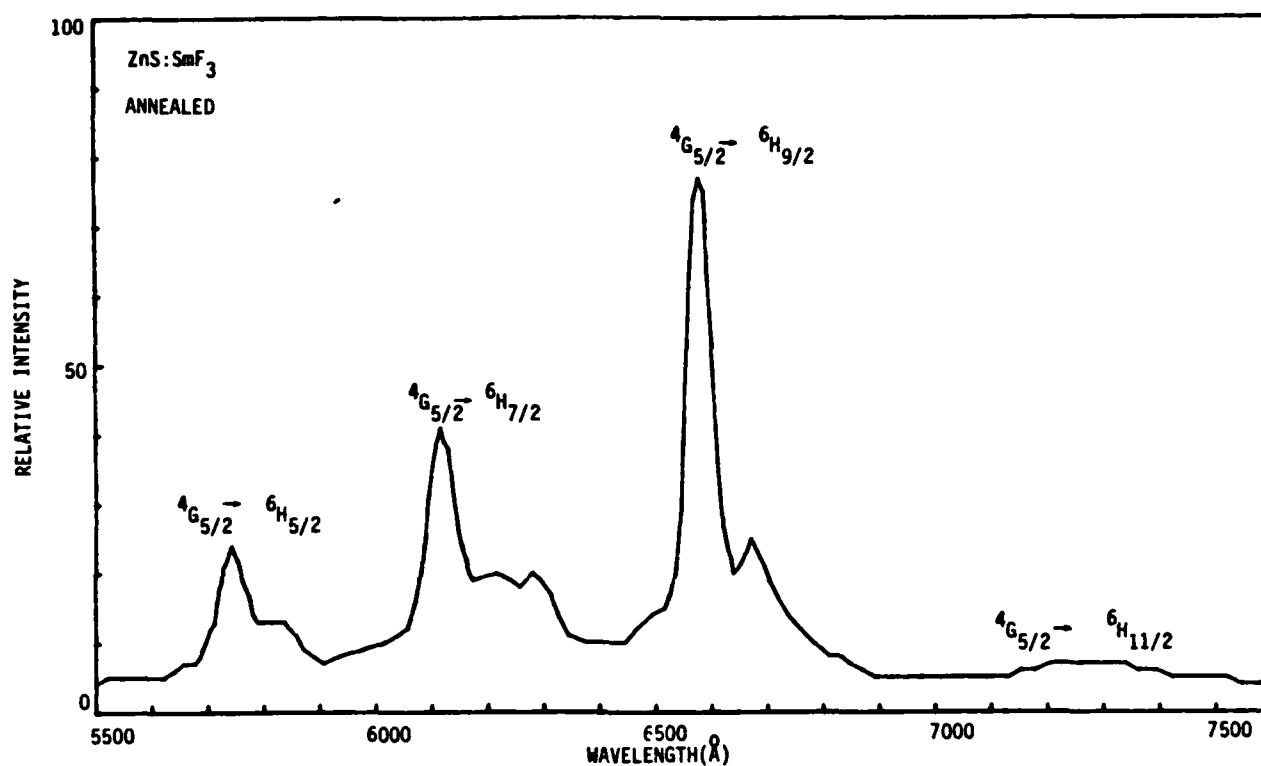


Fig. 2 Room temperature spectrum of an annealed ZnS:SmF₃ thin film emitter.



ERC41026.2FR

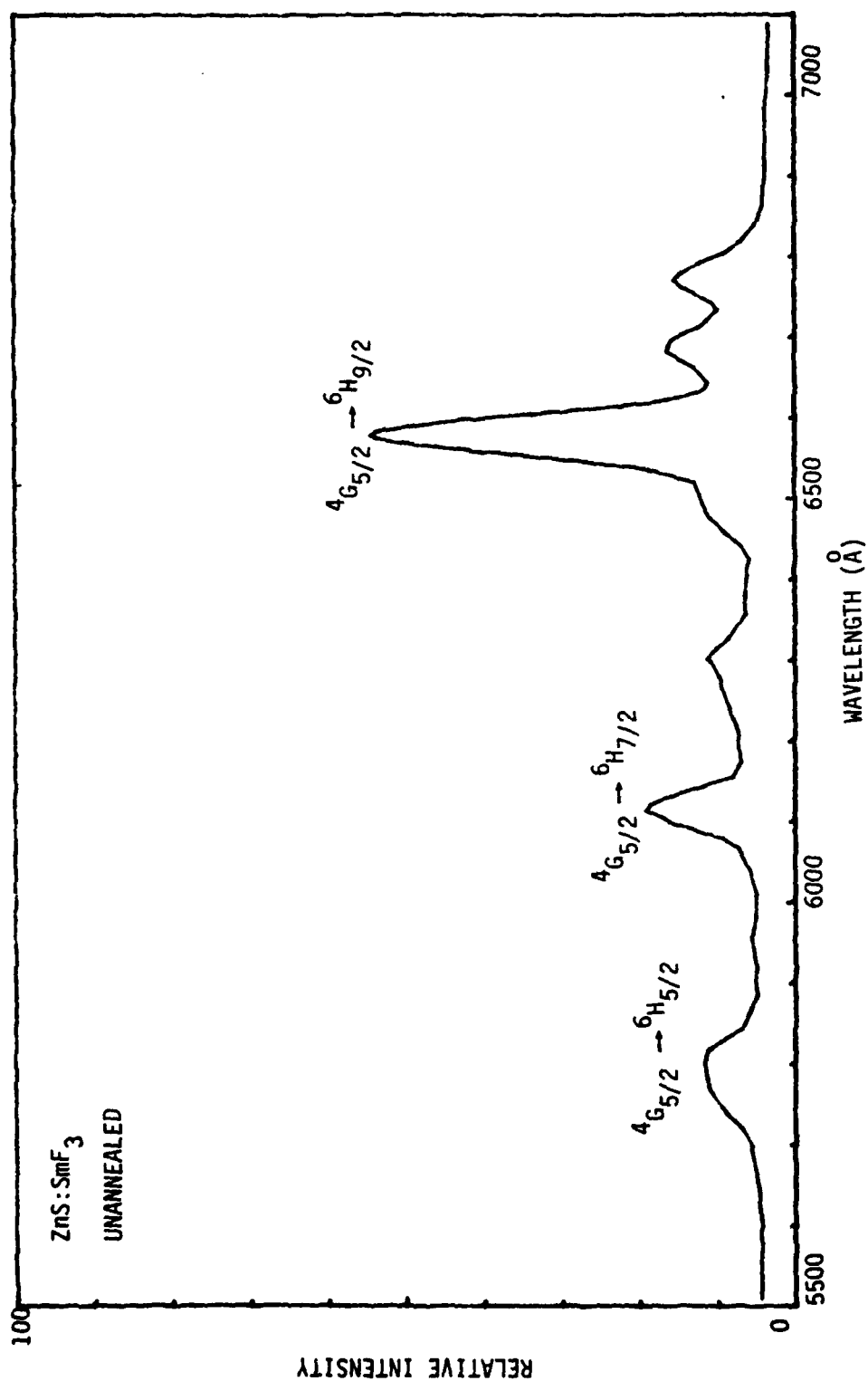


Fig. 3 Room temperature spectrum of an unannealed ZnS:SmF₃ thin film emitter.



compared between annealed and unannealed films, it is observed to decrease for the annealed films. This seems to imply that the Sm^{+3} ion occupies a site with greater symmetry after anneal. The ratio of these two transitions did not appear to change as a function of applied field. This latter observation is in contrast to what was observed for Tb^{+3} activated films. With the Tb^{+3} films the ratio of the blue to green transitions decreased with applied field indicating the possibility the excited electrons in the Tb^{+3} were decaying nonradiatively from the high energy level to the next lower level before emitting in the green region. This is discussed in more detail in the section on TbF_3 films. With the samarium films all transitions appear to increase uniformly with applied field. The result shows that the available energy is spread over a larger portion of the visible spectrum creating a red orange emission.

Figure 4 shows the decay time of a $\text{ZnS}:\text{Sm}^{+3}$ film which has been excited with square voltage pulse 45 μs wide. The time constant for the film is about 30 μs and this constant is defined as time to reach 1/3 of the peak value. From reports in the literature,⁸ this time constant appears very short. Previous experience with Mn^{+2} activated ZnS films indicate that the time constant is a function of the activator concentration.⁵ Short time constants are indicative of high concentrations. This observation is supported by Auger spectroscopic data indicating the concentration to be about 5%. High concentrations of activator ions tend to quench the emission.^{6,9} Efforts are continuing to determine the optimum concentration for these thin film emitters.

There have been recent reports which describe the rare-earth fluorides as acting as complex centers strongly linked to the ZnS matrix.¹⁸ These complex centers have an emission spectrum that is different than the rare-earth ion incorporated by itself in the ZnS lattice. An investigation was made to see if incorporating the samarium as a sulfide rather than a fluoride would change the emission.



Rockwell International

ERC41026.2FR

SC81-15584

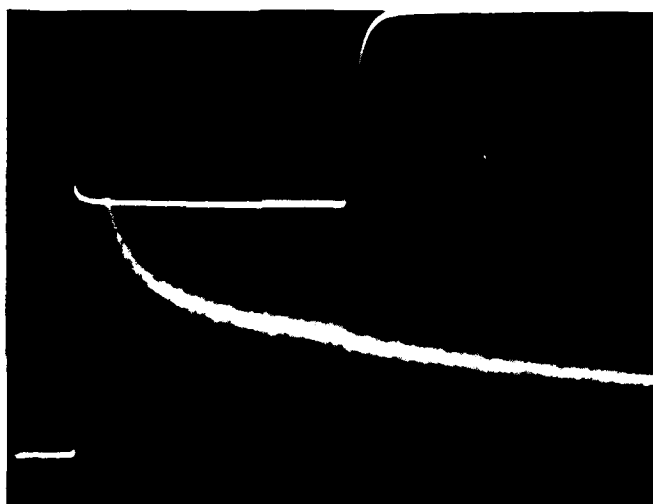


Fig. 4 Decay time of ZnS:SmF_3 film (a) upper trace; voltage pulse,
(b) lower trace; light output.



ERC41026.2FR

Figure 5 is the room temperature spectrum of a thin film emitter in which the starting activator was Sm_2S_3 . The same three transitions associated with Sm^{+3} appear in this spectrum. The decay time constant of 6 μs indicates a large concentration of Sm^{+3} (about 5%). Because of the high melting temperature of this material, it required an E-beam to evaporate. Normally, the activator is evaporated simultaneously with the ZnS from a resistance heated boat. This produces a layer with the activator distributed throughout the ZnS. In this latter configuration, we were able to monitor the activator and ZnS simultaneously during evaporation. During the Sm_2S_3 deposition, first a layer of ZnS was deposited, then a layer of Sm_2S_3 . This was repeated twice more and then the final layer was ZnS. With this multilayer structure, the thin layers of Sm_2S_3 were difficult to control. The result was a large samarium concentration (~5%). The decay time graph (Fig. 6) shows the double slope associated with quenching of emission. This multilayered structure required a longer annealing time (rediffusion of activator). Even with the longer anneal time, the samarium does not appear to have diffused out uniformly as seen from the depth profile of Fig. 7. In addition, the depth profile shows some residual yttrium in the active layer. Presently, it is not clear whether this is real or an instrumental error.

The results of the experiment are somewhat uncertain due to the difficulty in making the film and the resultant high concentration of activator. However, there does not appear to be any significant difference between the spectra of the SmF_3 and Sm_2S_3 films.

The room temperature spectrum for a Eu^{+3} activated film is shown in Fig. 8. This spectrum shows the expected transitions for the Eu^{+3} ion.⁷ The dominant transition is the $^5\text{D}_0 \rightarrow ^7\text{F}_2$ (6110Å) which is an electric dipole transition. There were two transitions below 5000Å which were very weak indicating that there was some Eu^{+2} . The intensity of the $^5\text{D}_0 \rightarrow ^7\text{F}_2$ and $^5\text{D}_0 \rightarrow ^7\text{F}_4$ transition indicate that the Eu^{+3} ion is located at a site without inversion symmetry even after anneal. This is contrary to results with samarium. Some films have been produced which have blue emission indicating the activator is



ERC41026.2FR

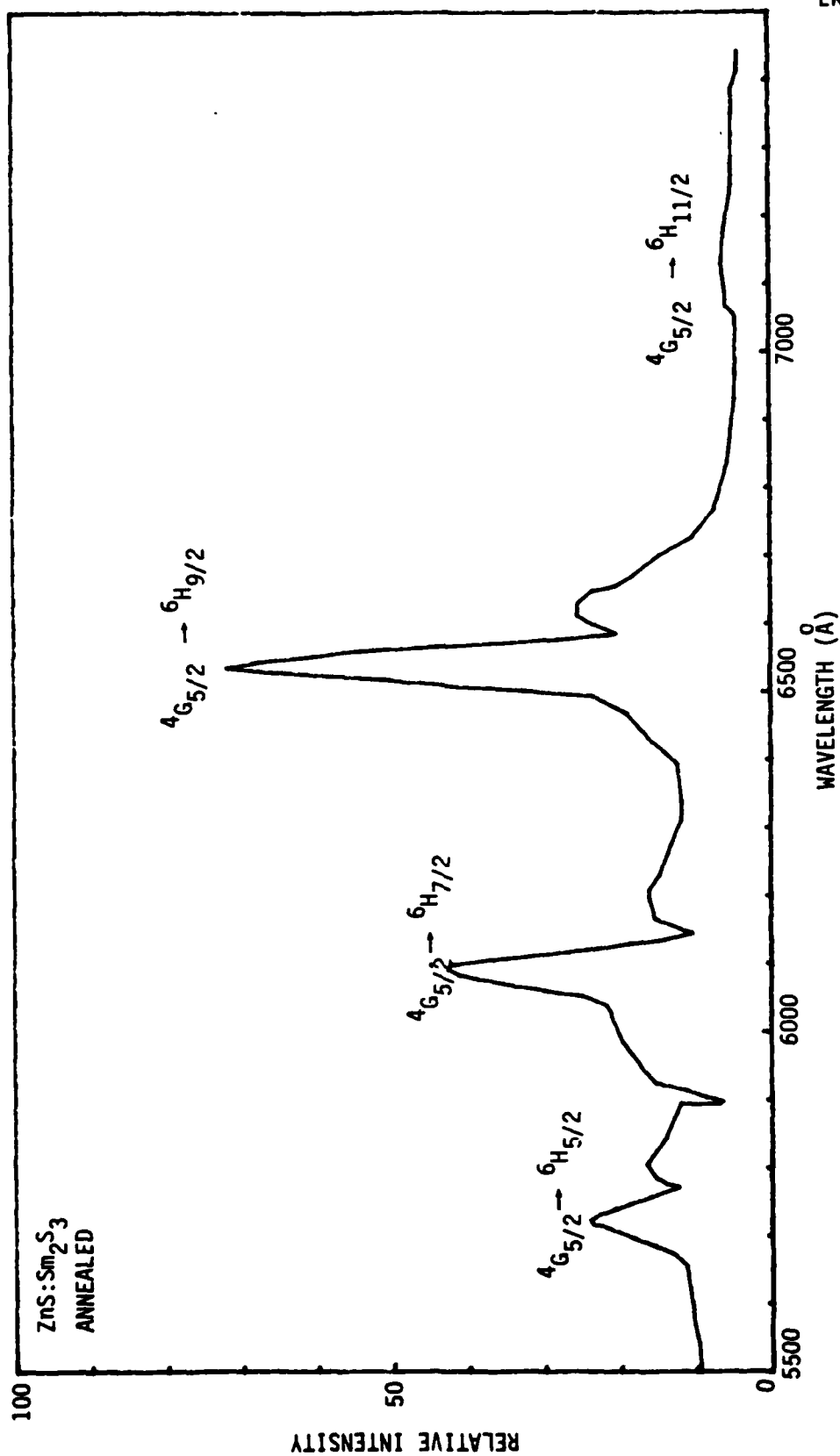


Fig. 5 Room temperature spectrum of ZnS:Sm₂S₃ thin film emitter.

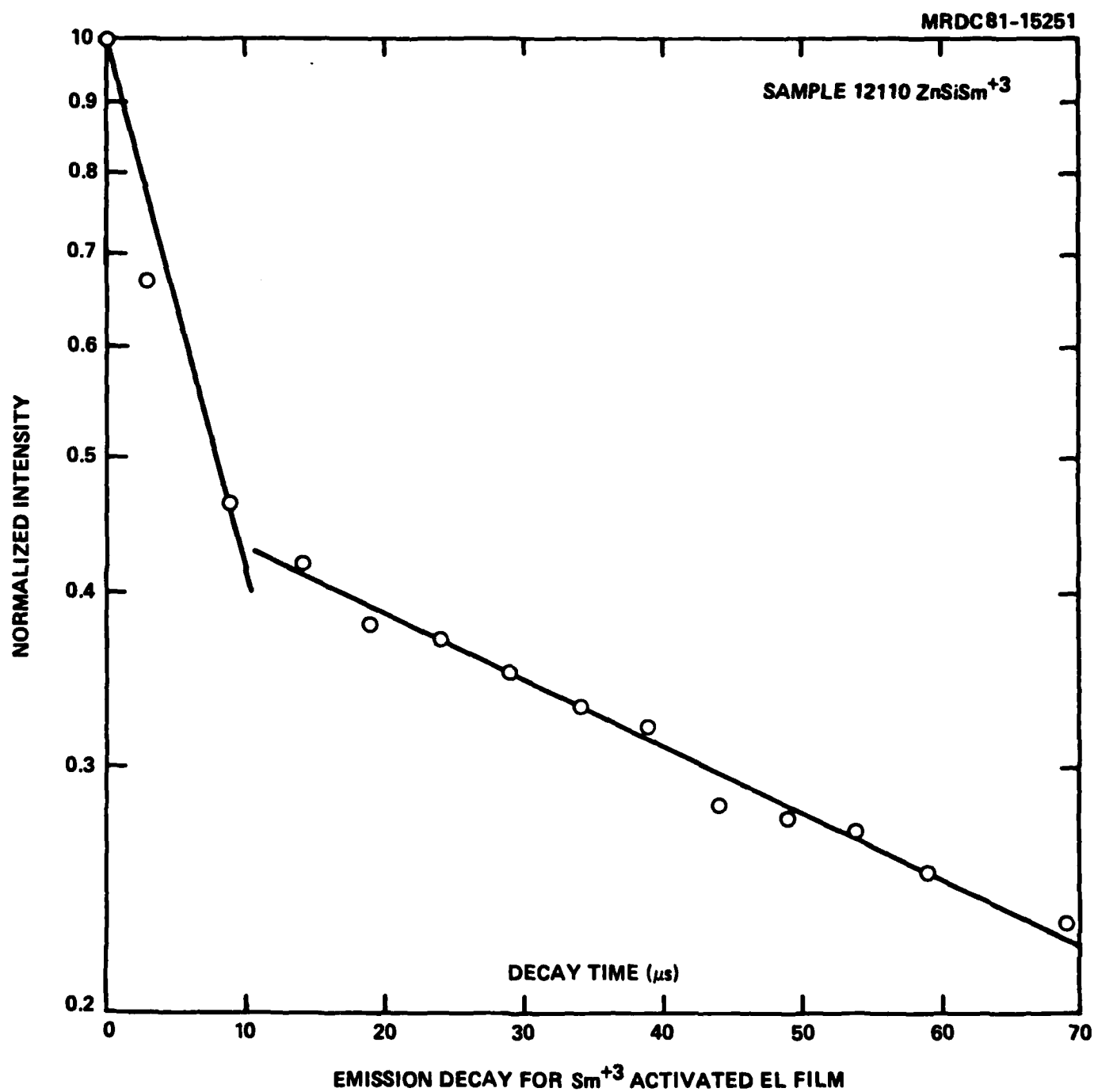


Fig. 6 Decay curve for ZnS:SmF_3 showing double slope.

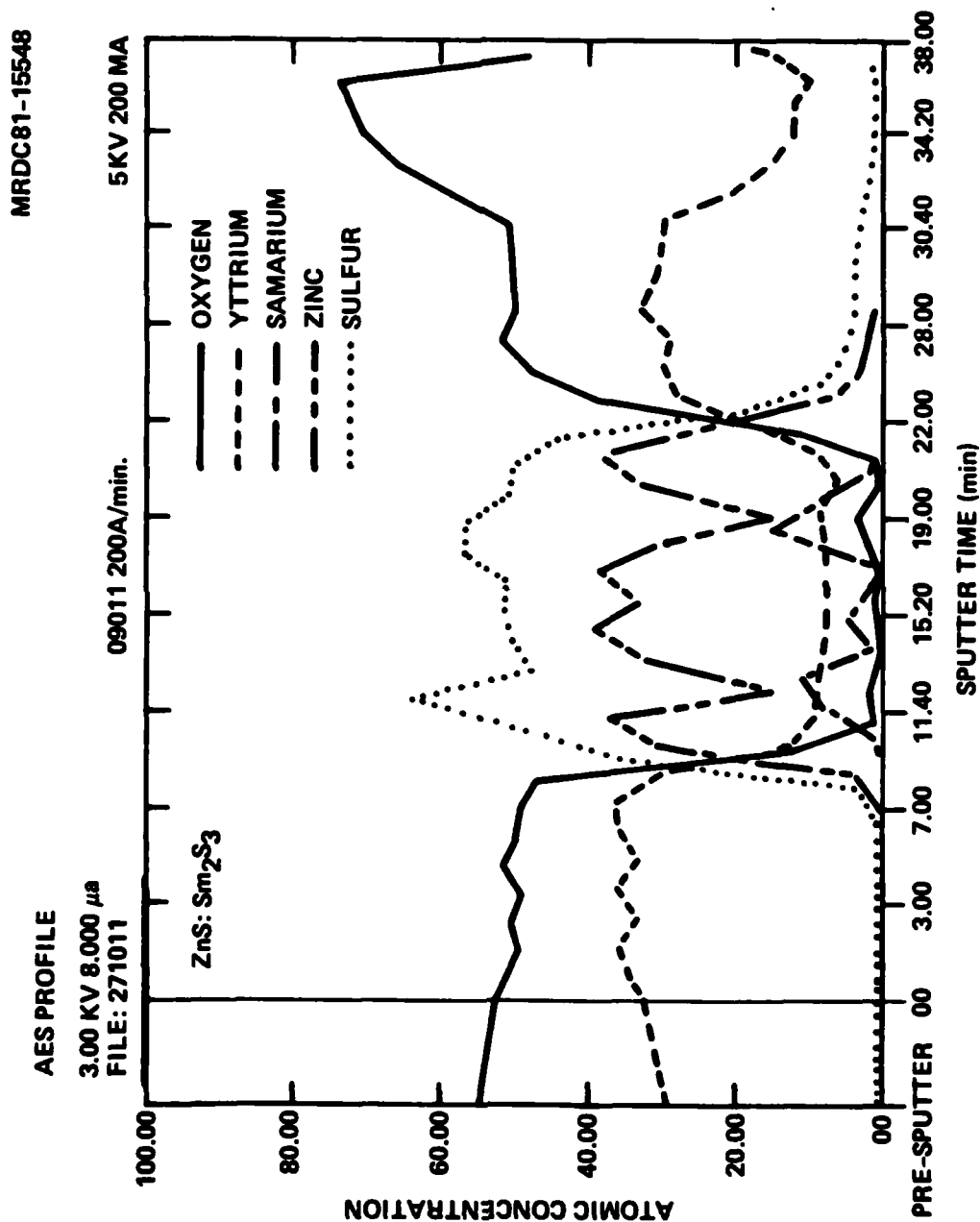


Fig. 7 Auger depth profile of ZnS:Sm₂S₃ thin film emitter.



ERC41026.2FR

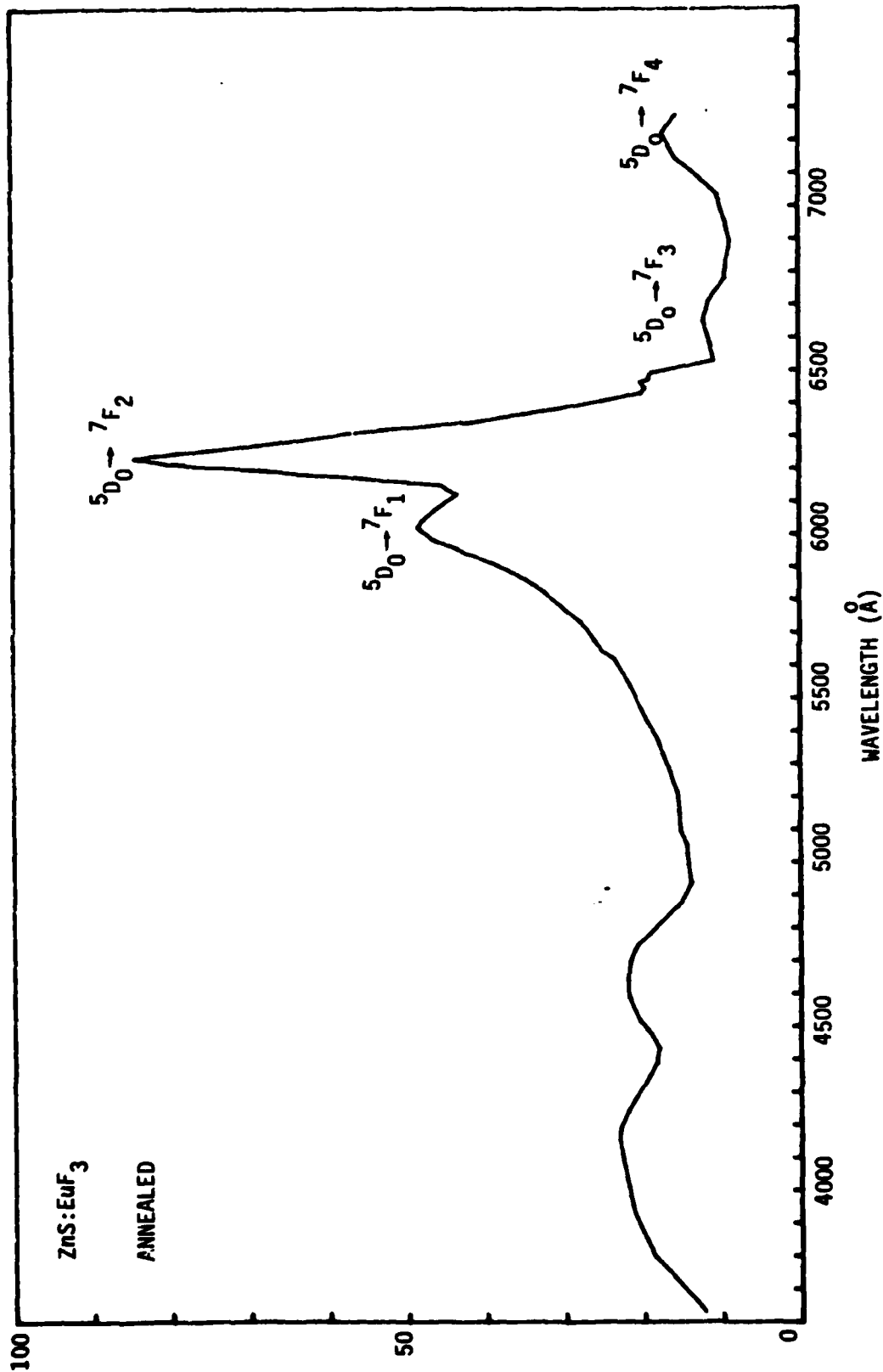


Fig. 8 Room temperature spectrum of ZnS:EuF₃ thin film emitter.



in the Eu^{+2} state. The brightness was very weak for all the europium activated films. The time constant for these films are 6-10 μs indicating a large concentration of activator.¹⁰

The room temperature electroluminescence spectrum of a ZnS:TmF_3 film emitter is shown in Fig. 9. The spectrum is somewhat different from that reported in the literature in that the transition at 6500A ($^1\text{G}_4 \rightarrow ^3\text{H}_6$) is missing. There is a rather broad peak at about 5800A which is presently not well understood. The dominant line is due to the $^1\text{G}_4 \rightarrow ^3\text{H}_6$ electric dipole transition center at 4800A (blue). The time constant for these films was 5 μs , which corresponds to the published results.⁸ The brightness of these films were about 1 fL.

It should be noted that the red and blue emissions occur at the tails of the photopic response of the eye (see Fig. 10). At the wavelength of the samarium emission, the eye is only 10% as sensitive as it is at its peak of 5500A. The eye's response is down to 50% at 6100A, the dominant peak for the Eu^{+3} emission and 14% for the thulium emission. The dominant line for the terbium ion is 5425A and for the manganese ion it is 5850A; both of these lines are very close to the maximum response of the eye.

The electroluminescence spectrum of ZnS:TbF_3 is shown in Fig. 11. The spectrum has the characteristic appearance associated with ZnS:TbF_3 reported in the literature.^{5,7} However, there are some differences. A comparison of the two spectra in Fig. 11 shows the high energy transition ($^5\text{D}_3 \rightarrow ^7\text{F}_5$) to be less intense for the films reported here. This result will be discussed shortly. The dominant line for these thin film emitters is the 5425A ($^5\text{D}_4 \rightarrow ^7\text{F}_5$) line. This is a magnetic dipole transition which implies that the Tb^{+3} ion occupies a site with inversion symmetry. The transition occurring at 4890A ($^5\text{D}_4 \rightarrow ^7\text{F}_6$) is an electric dipole transition ($\Delta J = 2$) which would normally be forbidden. The influence of the crystal field relaxes the selection rule for these transitions allowing them to occur, but with reduced intensities.¹¹ However, The designation of the site symmetry for Tb^{+3} ion can be misleading since in general this ion appears to be insensitive to the crystal field.¹¹

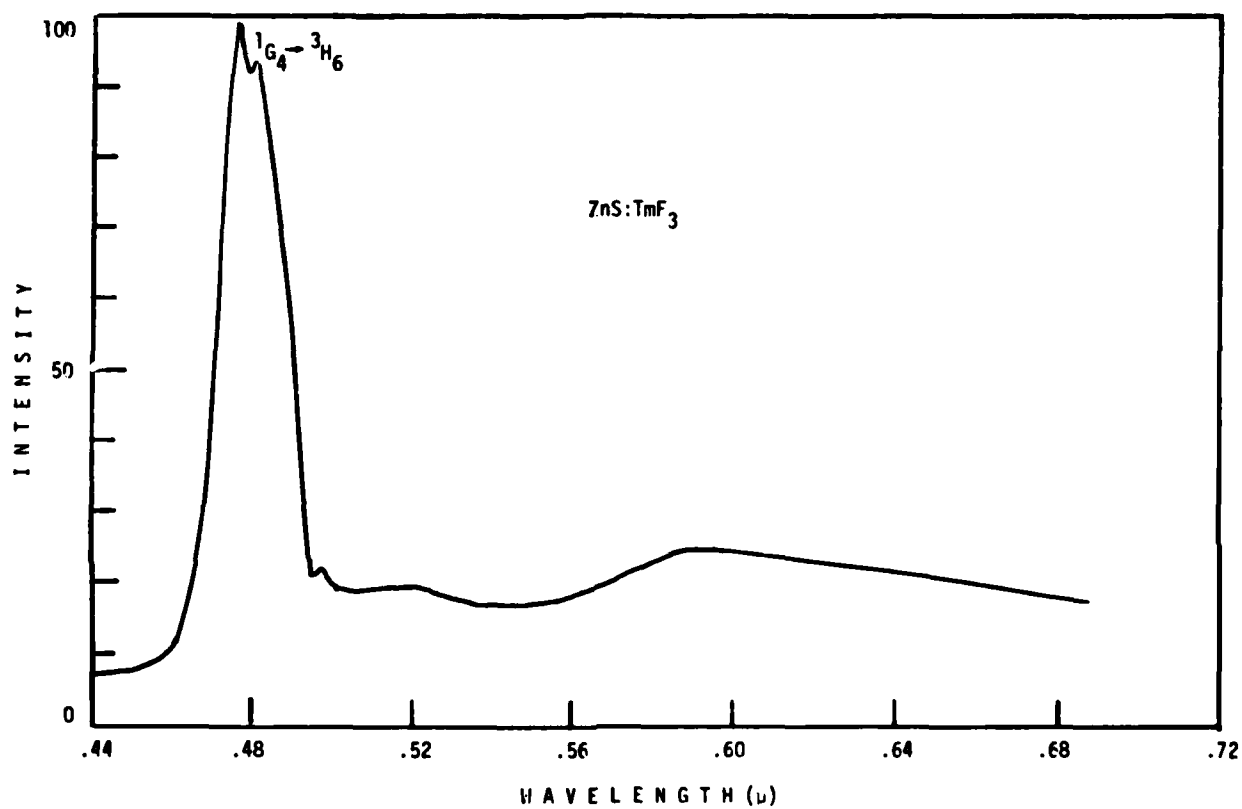


Fig. 9 Room temperature spectrum of ZnS:TmF₃ thin film emitter.

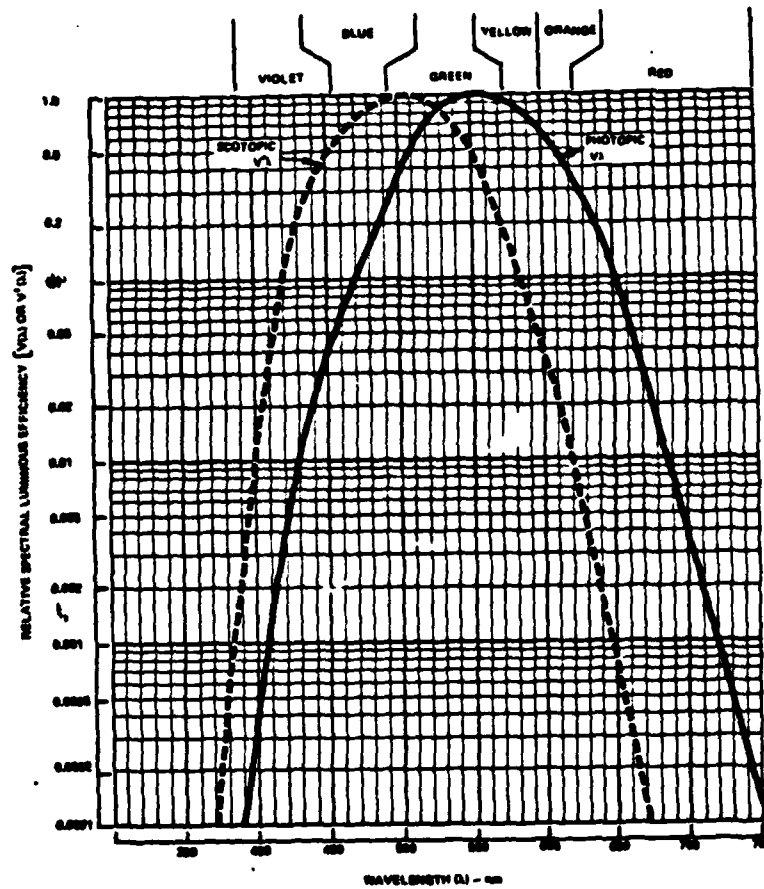
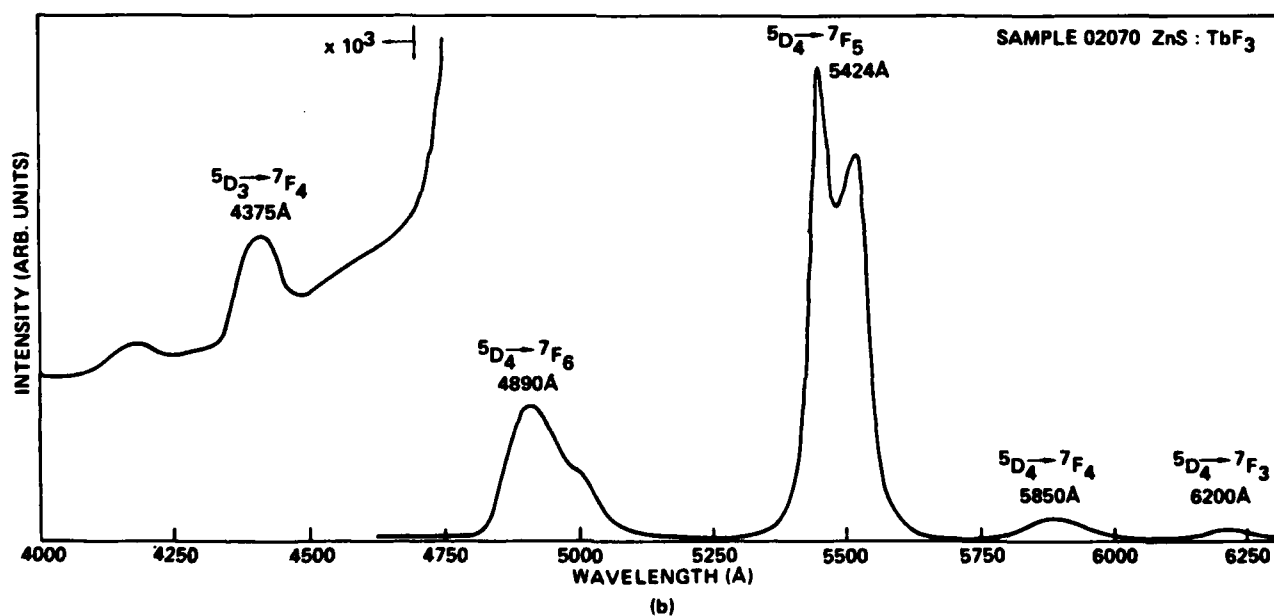
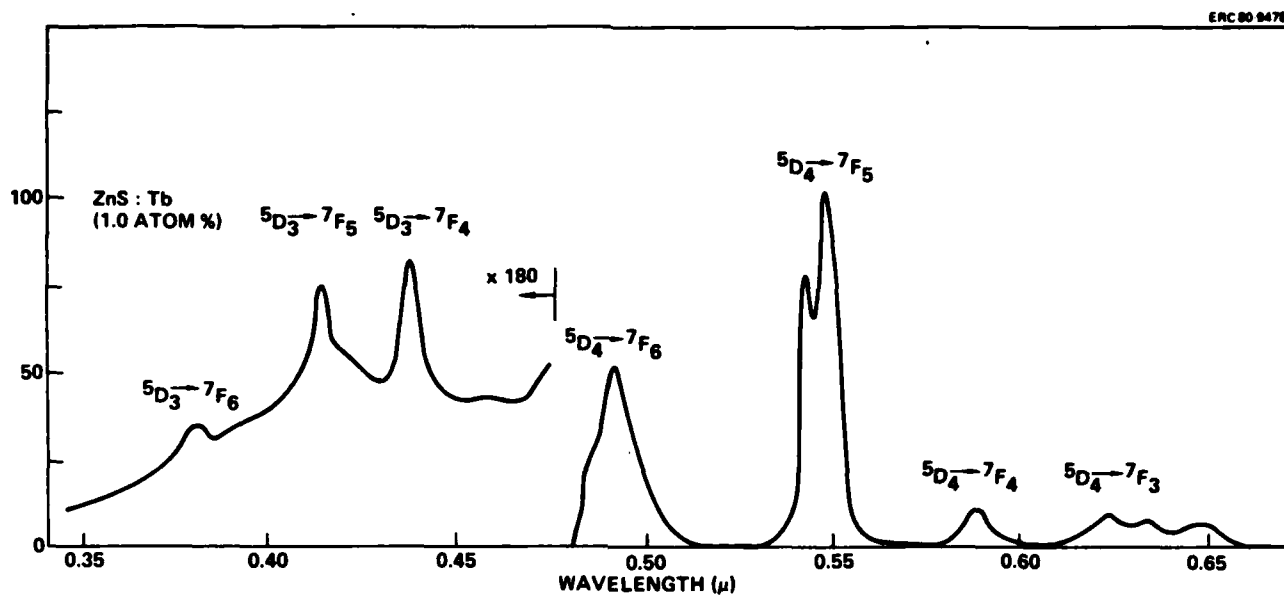


Fig. 10 Photopic response human eye.

Fig. 11 Room temperature spectrum of ZnS:TbF₃ thin film emitter.



It might be expected that as the field across the ZnS increases the energy of the electrons would also increase. In turn, this would increase the number of excitations to the higher energy 5D_3 level. If these decayed radiatively to the ground state then the ratio of the $^5D_4 \rightarrow ^7F_4 / ^5D_4 \rightarrow ^7F_6$ would increase with field. It was observed that this ratio decreased (see Fig. 12) and the ratio of the $^5D_4 \rightarrow ^7F_6$ to the $^5D_4 \rightarrow ^7F_5$ remained constant. This can be explained by assuming there were a significant number of nonradiative transitions from the 5D_3 to the 5D_4 level. This would increase the number of transitions from the $^5D_4 \rightarrow ^7F_6$ (4890Å) and the $^5D_4 \rightarrow ^7F_5$ (5425Å) level.

Brightness vs voltage measurements are made with a calculator controlled data acquisition system. Figure 13 shows a typical B-V curve for a Tb^{+3} activated ZnS layer. Also shown in Fig. 13 are the most recently published report of thin film $ZnS:TbF_3$ by Okamoto et al.¹² The films developed under this contract have a maximum brightness 3-1/2 times greater and a peak drive voltage that is 1.7 times lower. It should be noted that the brightness is plotted on a log scale. The steep nonlinear response indicates that the same mechanism responsible for emission in Mn activated devices is dominant in the Tb devices. This mechanism can be explained as follows: charges from deep traps within the active layer are field ionized and swept to the interface between the dielectric (Y_2O_3) and the ZnS layer where they are trapped. In the next voltage cycle they remain in their traps until the field reaches a sufficient level to allow the charges to tunnel through the barrier and become "hot electrons" very fast. These energetic electrons then impact, excite the activator causing luminescence, and are trapped at the opposite interface where they remain until the next half cycle of the voltage waveform. The process then repeats itself. It is this tunneling field emission which explains the steep nonlinear characteristics of these thin film emitters.

Electron injection by tunnel emission into the ZnS provides a distinctly different electro-optic response for thin film emitters compared with previous devices using bulk powder phosphors. Tunnel emission is insensitive to temperature and is sharply dependent on electric field strength. The

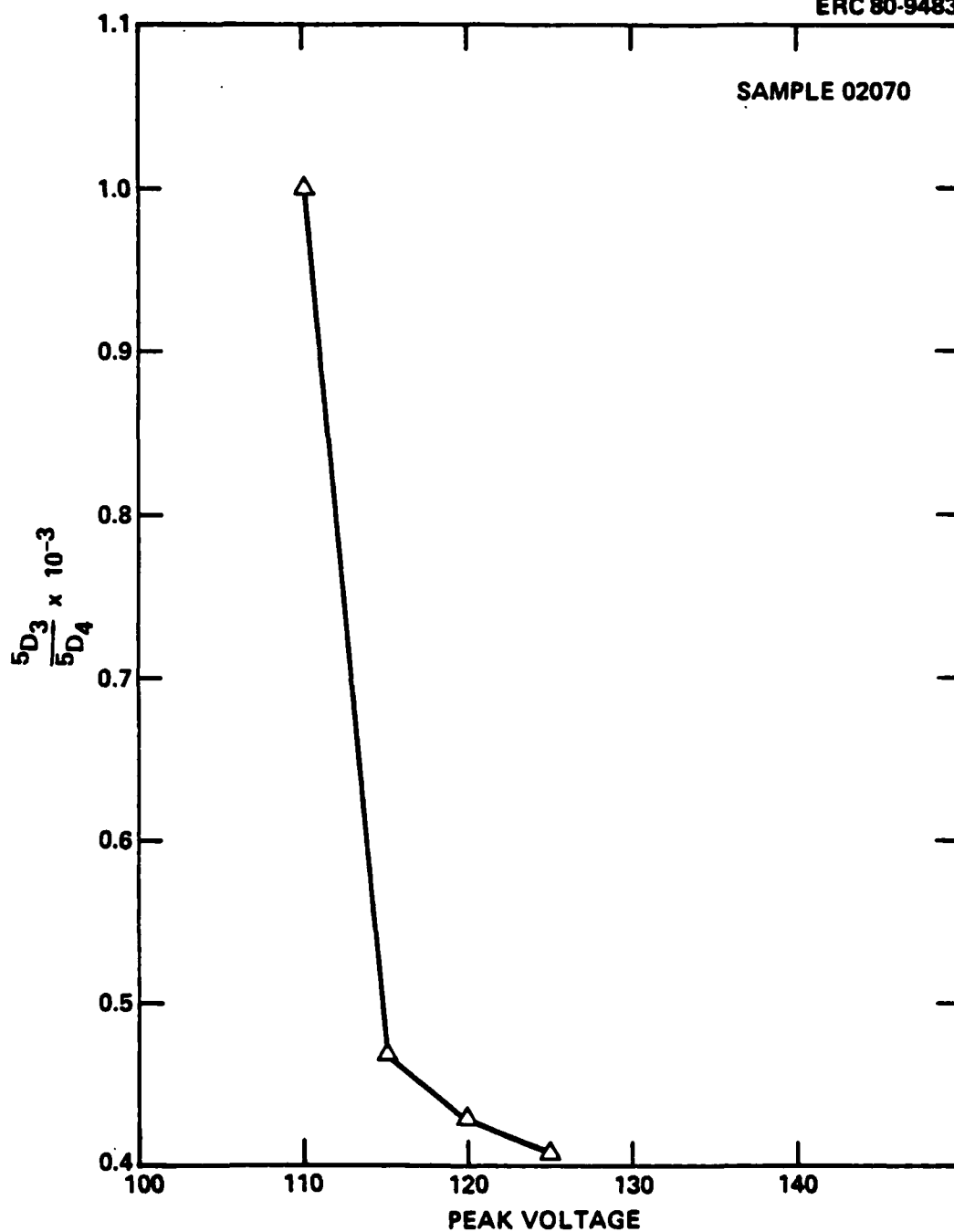


Fig. 12. Ratio of $5D_3 + 7F_4 / 5D_4 + 7F_6$ transitions vs applied field for ZnS:TbF₃ film.



ERC41026.2FR

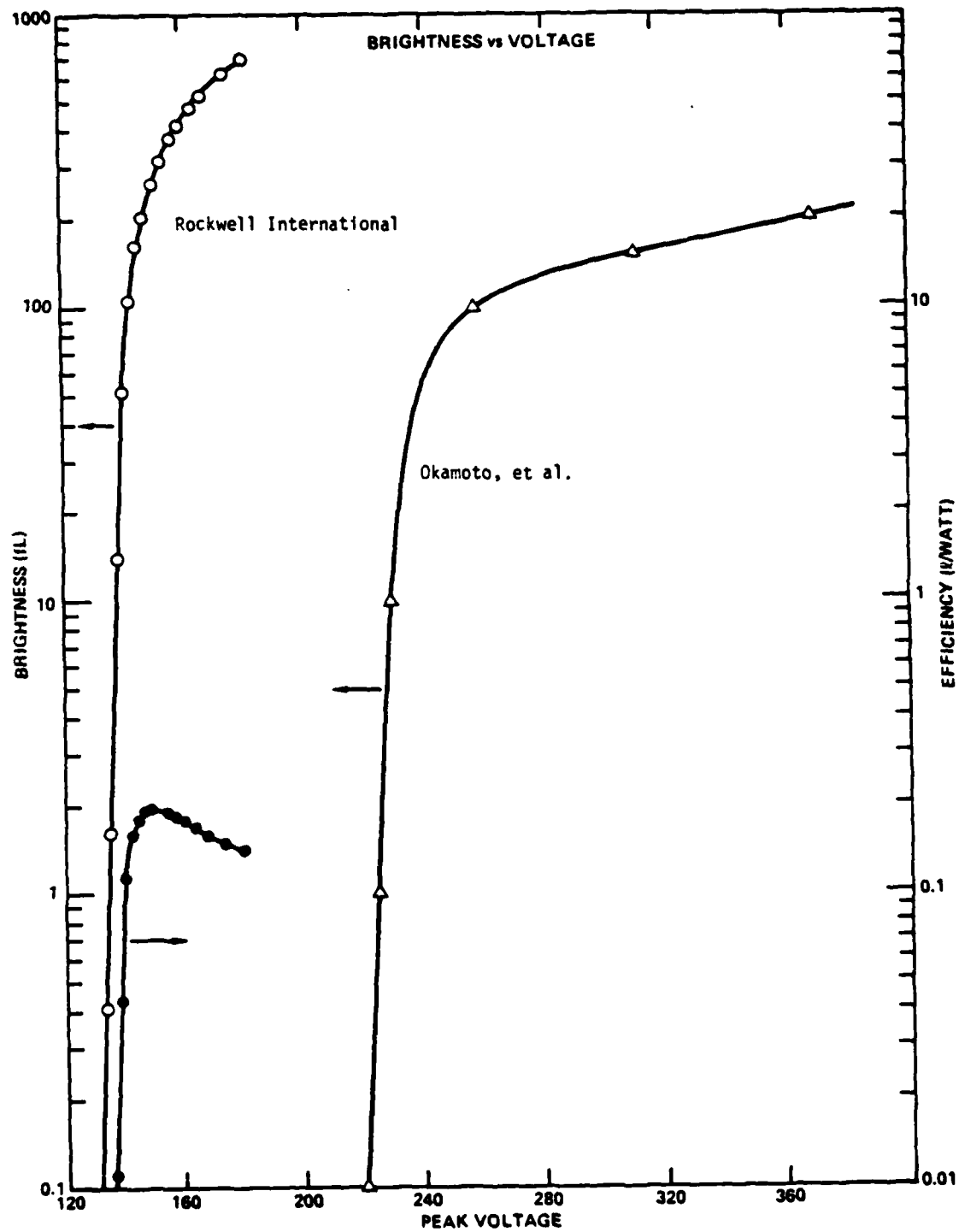


Fig. 13 Brightness vs voltage results of this program compared to published reports.



expression for the current density is

$$j(t) = n_1 v (E_1) e^{-AE_1^{3/2}/F}$$

n_1 = density of electrons in trap E_1

v = vibrational frequency of electrons in traps

E_1 = energy of trapping level

F = electric field across active layer

A = constant.

The brightness which is proportional to the tunneling current, therefore, is very nonlinear with respect to the voltage on the device. The validity of the model for Mn activated films has been reported previously.¹³ This nonlinear electro-optic response is a function of the tunnel emission, due to the layered structure and not the activator.

Figure 14 shows a plot of $\log j_{\max}$ vs $1/F$ for a Tb activated sample. The electronic current is found by placing a triangular voltage waveform across the device and monitoring the current. For a capacitor which exhibits no tunneling, the current waveform is a square wave. However, for a device in which there is a tunneling current, this current is superimposed on top of the square wave displacement current (see Fig. 15). The slope of the $\log j_{\max}$ vs $1/F$ curves gives the energy of the trap level (~ 0.9 eV). It can be seen from the figure that there appear to be two slopes. The bending of the curve at higher voltages is due to polarization charge which is building up at the opposite interface. This polarization produces a field which opposes the internal field across the active layer. As the external field is increased, a larger proportion is dropped across the dielectric. The number of charges which appear at the opposite interface can be determined by integrating under the electronic current waveform. The change in field due to these charges is sufficient to cause the change in slope of the j_{\max} vs $1/F$ curve. Further evidence which shows that the polarization charge is responsible for the change in slope is seen in Fig. 14 where the frequency has been increased to 5 kHz and the change in slope is less. Similar results have been reported by this laboratory in the past for Mn films.¹⁴



ERC41026.2FR

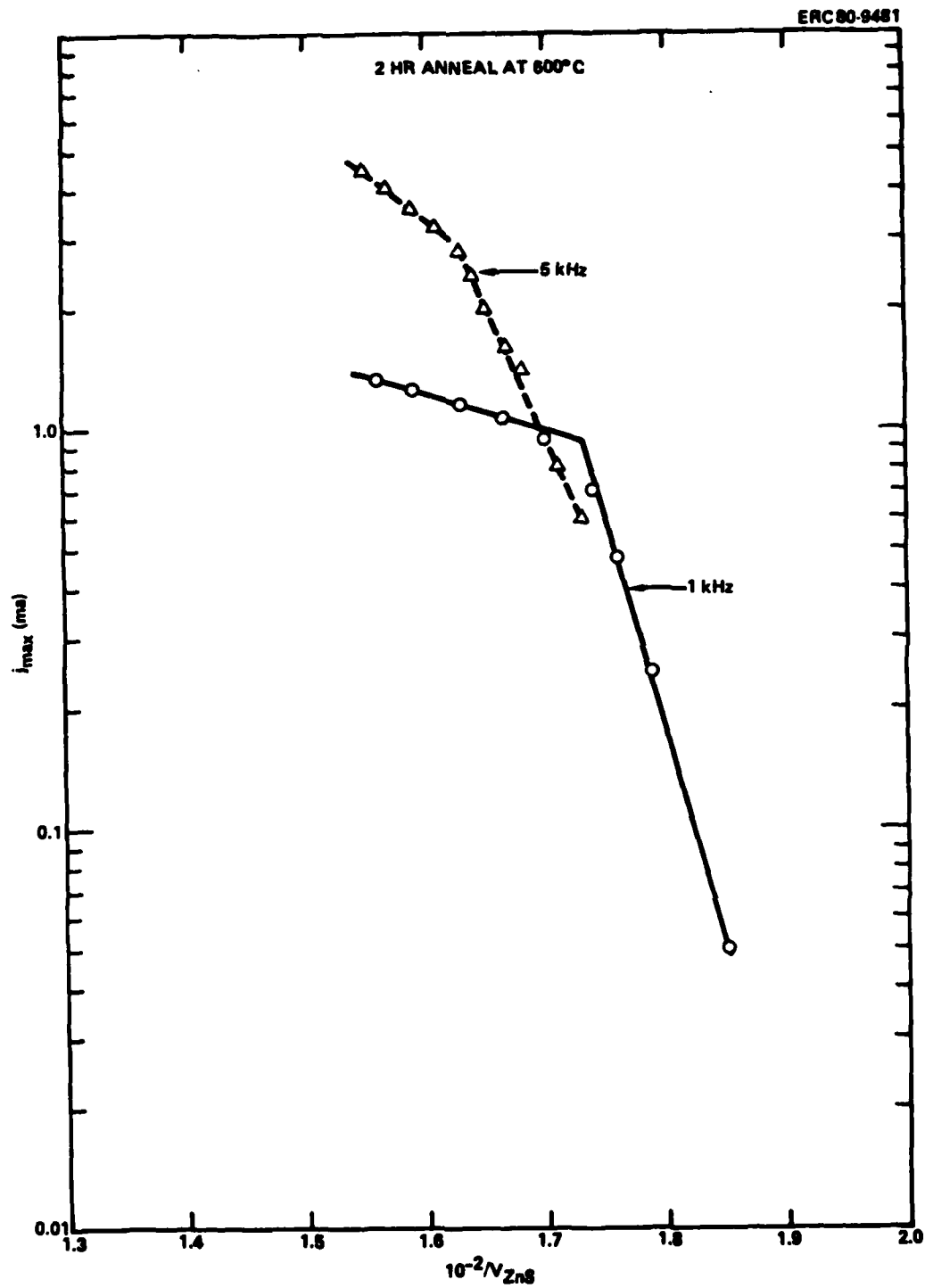


Fig. 14 Electronic current vs (field across ZnS)⁻¹ for ZnS:TbF₃ thin film.



ERC80-9475

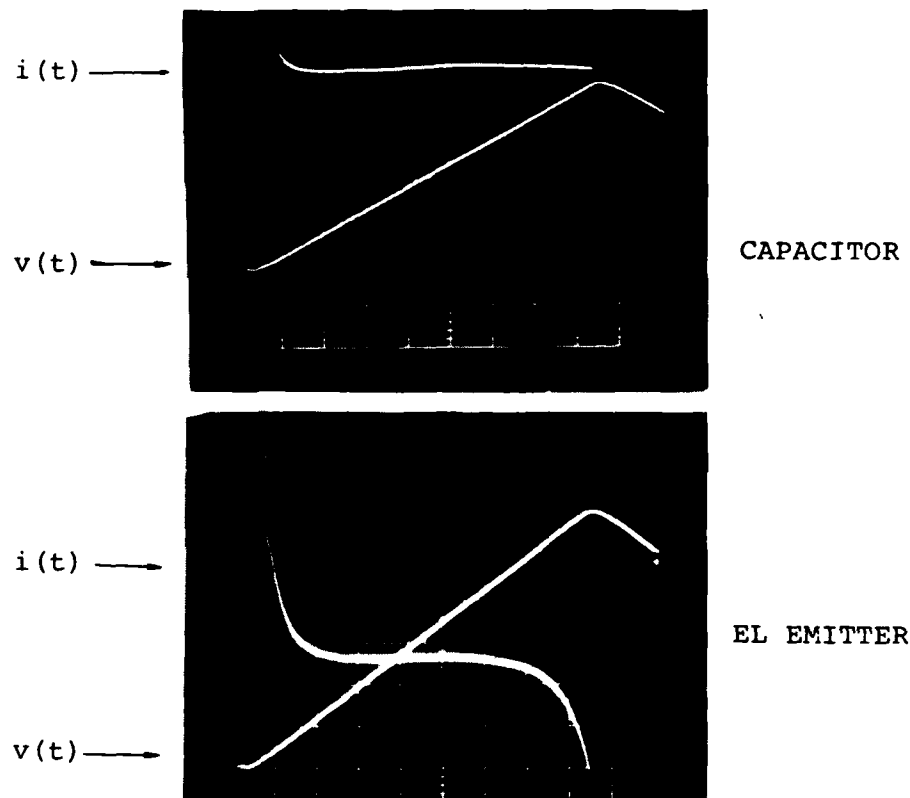


Fig. 15 Technique for separating electronic current from displacement current.



ERC41026.2FR

The luminous conversion efficiency is also shown in the same Fig. 13. The efficiency is determined by sampling the voltage waveform across the device and the current through the device. The average power consumed by the device is calculated by integrating the product of the two functions over the period of the waveform. The luminous conversion efficiency is then calculated knowing the average brightness and the area of the emitter. This is all accomplished with the HP 9825 calculator.

Figure 16 shows the decay characteristics of a typical Tb activated EL film. The luminescence decay consists of at least two exponential components. This has been explained in the literature as due to the formation of activator complexes as the concentration is increased. The longer time constant is associated with isolated activator centers and the faster time constant is associated with complexes.^{6,15} This is particularly true for manganese activated thin films and also appears possible for the terbium films. Further work is needed in this area. If complexes are being formed as the activator concentration is increasing, this is probably influencing the maximum efficiency. The time at which the intensity falls to $1/e$ of its initial value is $380 \mu s$. Previously reported values were $220 \mu s$ Chen et al⁸ and $700 \mu s$ Okamoto et al.¹² The decay time of a typical Mn activated film is included in Fig. 16 as a comparison.

Figure 17a, b, c, d shows the effect of annealing a device at constant temperature for different times. The plots show that the luminous conversion efficiency remained constant whether the device was annealed or not. The fact that the two hour anneal increased the maximum light out and current density indicates that this particular time-temperature cycle increased the number of charges available to produce light. However, since the conversion efficiency did not change the nonradiative decay mechanisms were not affected. This implies there is a better anneal temperature since results with Mn activated films indicates that annealing improves both the maximum light out and the efficiency. With the Mn films annealing tends to make the film more crystalline which increases the mean free path of the hot



ERC41026.2FR

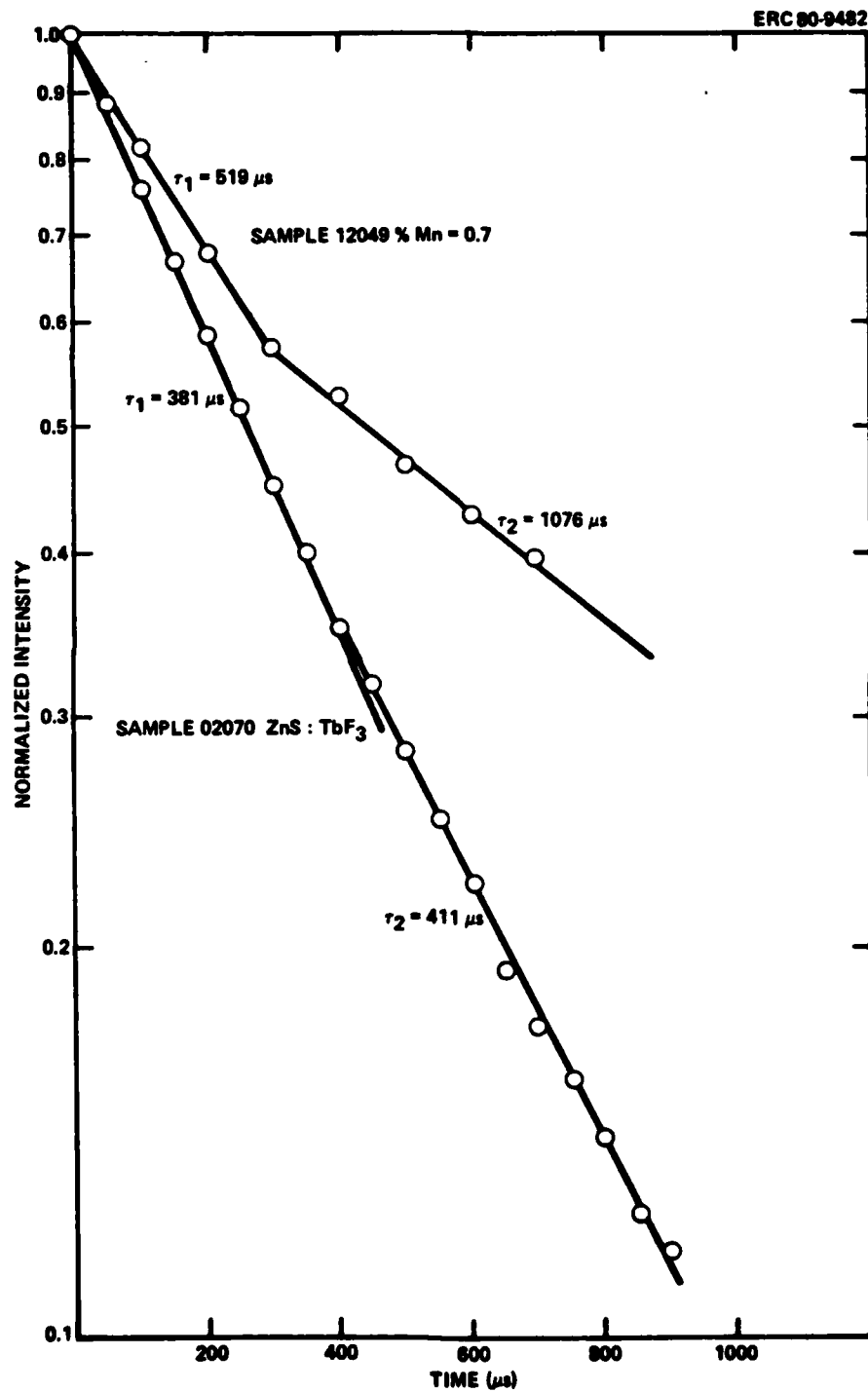


Fig. 16 Decay curve for ZnS:TbF₃ thin film showing double slope.

ERC41026.2FR

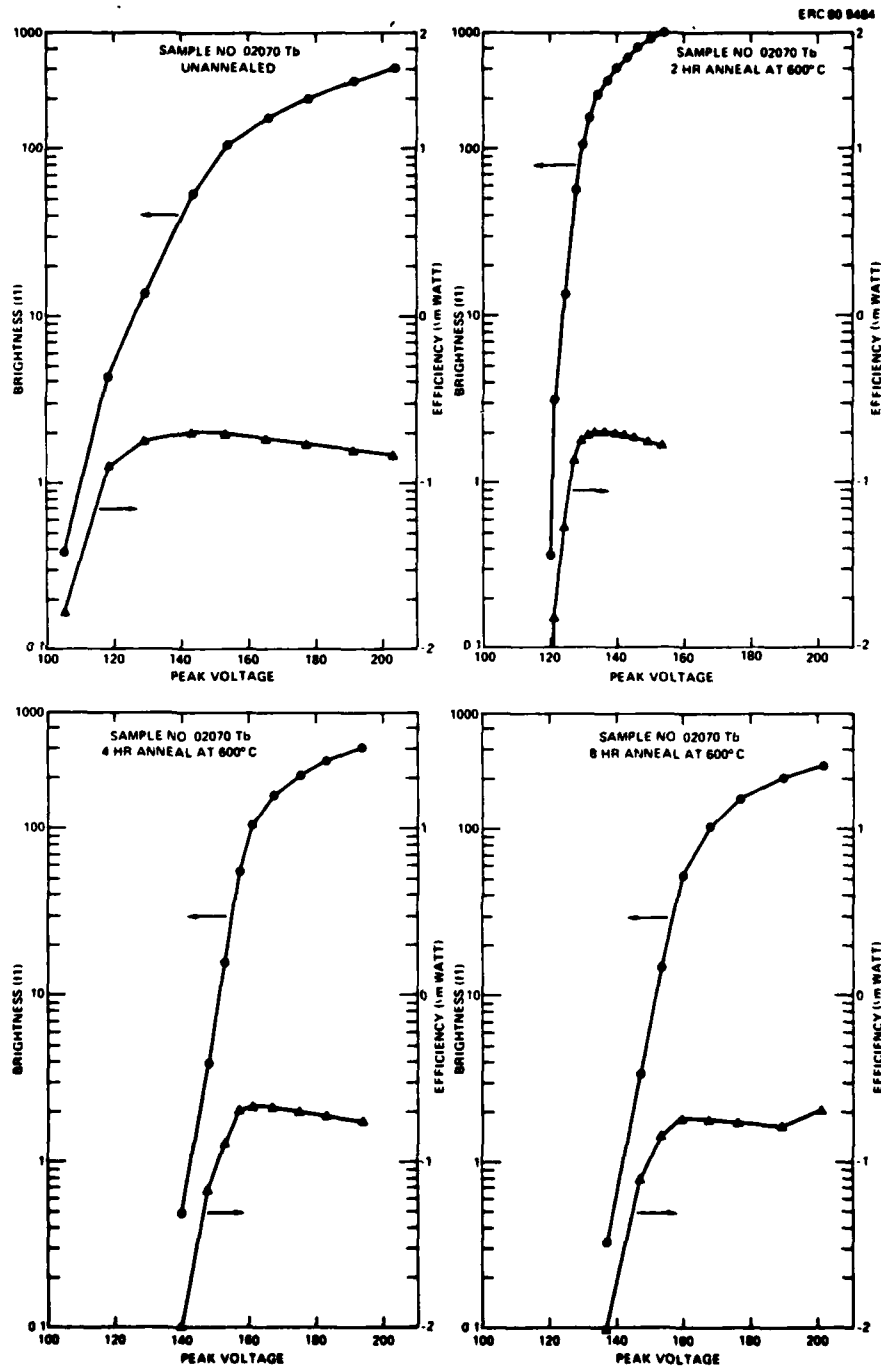


Fig. 17 (a), (b), (c), (d). Effect of annealing ZnS:TbF₃ thin film emitter at constant temperature for different times.



electron. The maximum power efficiency is determined by the product of the electric field across the active layer and the mean free path of the electron.¹⁶ Electron spin resonance experiments done at this laboratory have shown that annealing Mn activated films causes localized Mn^{+2} ion to diffuse so that they are more homogeneously distributed in the lattice.

The brightness-voltage curves for the $ZnS:SmF_3$ and $ZnS:TmF_3$ thin film emitters are shown in Figs. 18 and 19. The films exhibit the nonlinear electro-optic response associated with the electron injection rather than from the activator.¹³ The brightness of the Eu^{+3} activated film was less than 0.1 fL. Our experiments with rare earth activators indicate that red and green thin film EL emitters are possible. The green film produced in this laboratory has the highest brightness reported to date (700 fL).² The luminance of the red emitter needs improving. However, with further optimization of the concentration, we should be able to produce a red emitter with at least 50 fL. Note that the red emission occurs at the tail of the photopic response of the eye, hence at this wavelength the eye is only 10% as sensitive as it is at its peak of 5500Å. The dominant line for the Tb^{+3} ion is 5425Å and that for the Mn^{+2} ion is 5850Å, both of these are very close to the maximum response of the eye. The blue emitter appears more difficult to develop using ZnS host material. This is probably related to the solubility of the rare earths in ZnS.

Table I summarizes the results of the various activators investigated.



SAMPLE # = 12100-Sm

ERC41026.2FR

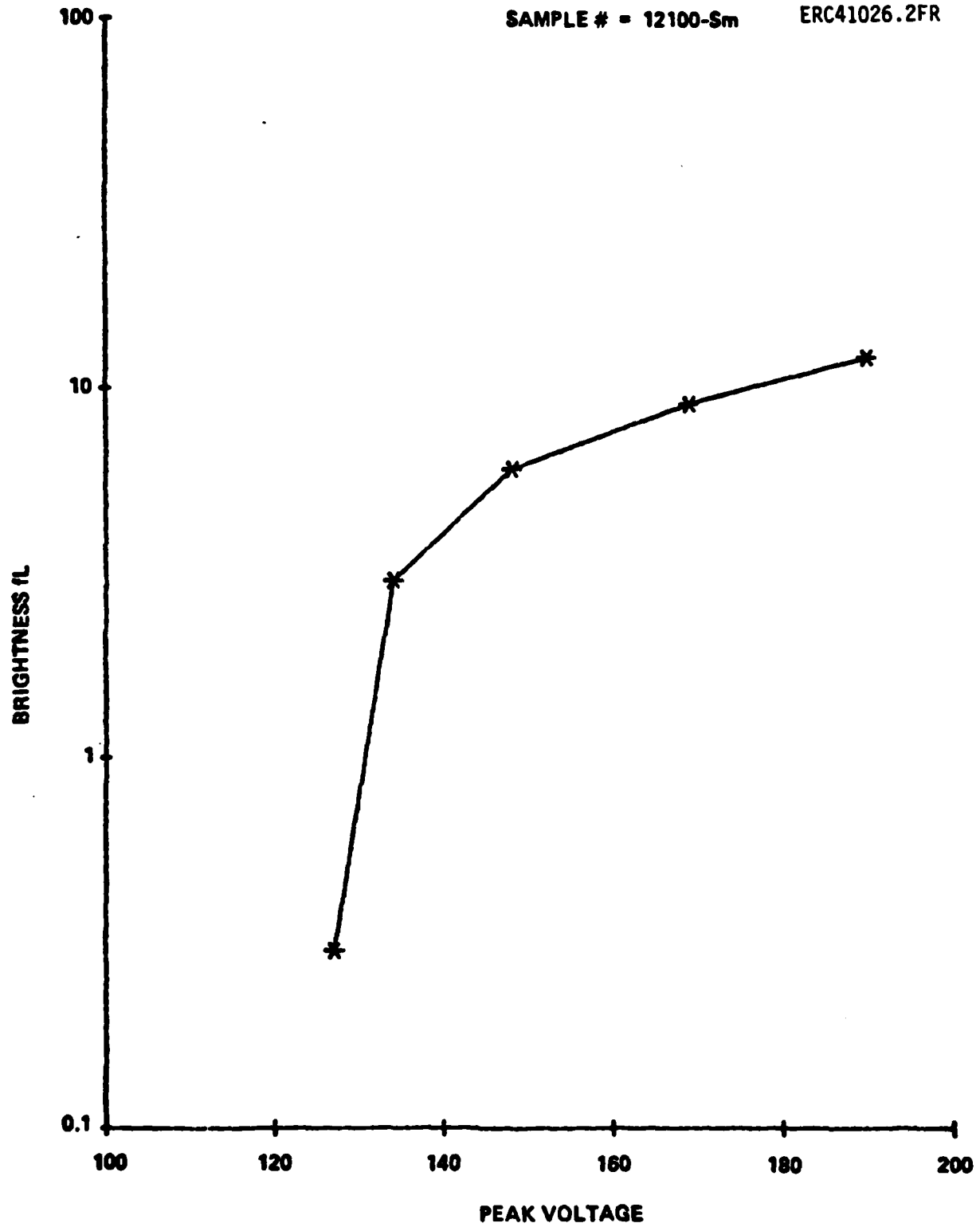


Fig. 18 Brightness vs voltage curve for ZnS:SmF₃ thin film emitter.



ERC41026.2FR

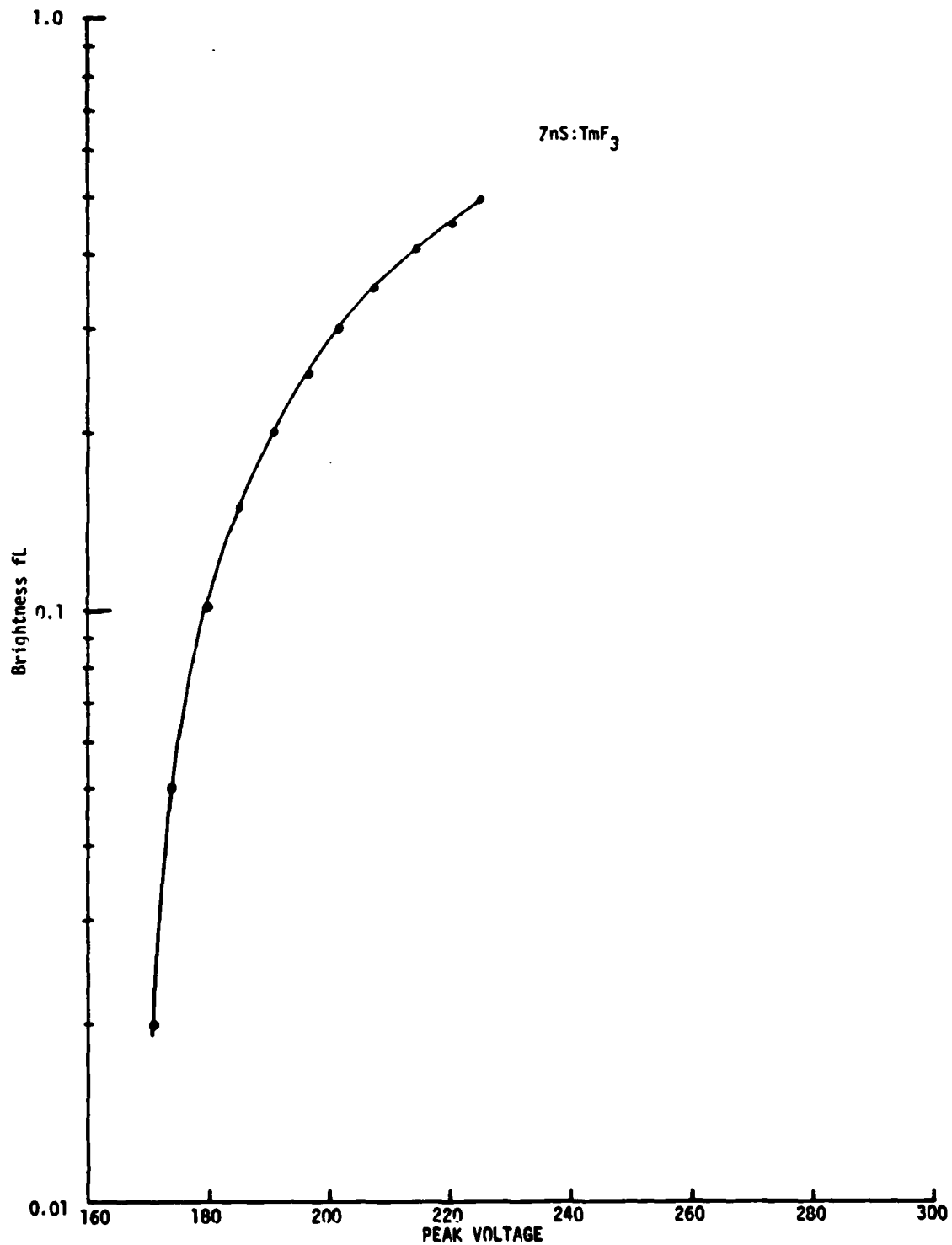


Fig. 19 Brightness vs voltage curve for ZnS:TmF₃ thin film emitter.



ERC41026.2FR

Table I

Electro-Optic Parameters of Rare-Earths Activated
ZnS Thin Film Emitters

| Activator | Max. Brightness | Decay (μ s) | Chromaticity Coordinates | |
|-----------|-----------------|------------------|--------------------------|------|
| | | | X | Y |
| Tb | 700 | 380 | 0.32 | 0.58 |
| Sm | 15 | 30 | 0.53 | 0.4 |
| Tm | 1 | 5 | 0.23 | 0.23 |
| Eu | <0.1 | <10 | | |



5.0 CONCLUSIONS

The objective of this contract was to investigate the feasibility of fabricating multi-color thin film EL emitters using rare-earth activators in a ZnS host. It has been found that the rare-earths Tm^{+3} , Tb^{+3} and Sm^{+3} can be incorporated into the ZnS matrix to produce blue, green and red thin film EL emitters. The terbium activated material has produced the brightest green thin film EL emitter (700 fL) reported to date. The two dominant transitions occur at 4890Å (blue) and 5425Å (green). The green line is approximately three and one-half times as large as the blue. With the proper filtering, the green line could be suppressed and a significant blue emission could be realized.

The high brightness of the terbium activated films could be due partially to the fact that the peak transition is located very close to the peak of the photopic response of the eye. In addition, the terbium ion appears to be less sensitive to site location within the crystal lattice.¹¹ That is, the magnetic dipole transition is the dominant transition regardless of site symmetry. This is not true for the other ions (Eu^{+2} , Tm , Eu^{+3} and Sm^{+3}) which were investigated. The anneal studies with terbium films indicate they appear to diffuse in the ZnS crystal more readily than the red and blue activators.

Further improvements of the red emission of the samarium films could be realized by optimizing the activator concentration and determining the best anneal cycle. However, a greater improvement in the red emission could be realized if europium (Eu^{+3}) could be incorporated into the ZnS lattice in a reproducible manner. This occurs because the narrow line emission of the Eu^{+3} ion at 6100Å is closer to the peak response of the eye. Therefore, the ratio of the luminous flux to the corresponding radiant flux is greater. A more stable Eu^{+3} film might be accomplished by incorporating the europium in the ZnS lattice as a sulfide rather than a fluoride.



ERC41026.2FR

The poor results with the thulium activated films are not well understood at present. Cathodoluminescent measurements on ZnS:Tm phosphors reported in the literature¹⁷ indicate that this activator should be a rather efficient emitter.

Recently, significant improvements have been reported in the efficiencies of CRT and lamp phosphors. The improvement is due to the implementation of rare-earth oxysulfide phosphors. Thin films of these materials have been deposited on CRT screens providing extremely good performance (40,000 fL).¹⁹ The oxysulfide materials appear to be excellent candidates for thin film ac electroluminescent emitters using the triple layer structure developed for the activated zinc sulfide phosphors.



6.0 REFERENCES

1. A. Brill and W. L. Wanmaker, "New Phosphors for Color Television." Philips Tech. Rev. 27(1), 22 (1966).
2. L. G. Hale et al, "Improved Green and Blue Thin Film Electroluminescent Emitters." Digest IEDM 1980, Washington, D.C.
3. L. G. Hale, R. Ketchpel and W. Hall, "Efficiency of Thin Film ac EL Emitters." Digest IEDM, 1979, Washington, D.C.
4. G. Blasse, "Materials Science in Luminescence," in Luminescence of Inorganic Solids (B. D. Bartolo, ed.), Plenum Press, New York, 1977, pp. 457.
5. D. C. Kurpka and D. M. Mahoney, "Electroluminescence and Photoluminescence of Thin Films of ZnS Doped with Rare-Earth Metals." J. Appl. Phys. 43(5), 2314 (May 1972).
6. J. M. Hurd and C. N. King, "Physical and Electrical Characterization of Co-deposited ZnS:Mn Electroluminescent Thin Film Structures." J. Electronic Materials 8(6), 879 (1979).
7. E. W. Chase et al, "Electroluminescence of ZnS Lumocen Devices Containing Rare-Earth and Transition-Metal Fluorides." J. Appl. Phys. 40(6), 2512 (1969).
8. Y. S. Chen, M. V. DePaolis and D. Kahng, "Characteristics of Pulse Excited Electroluminescence from ZnS Films Containing Rare-Earth Fluoride." Proc. IEEE 58(2), 184 (1979).
9. L. G. VanUitert, "Luminescence in Insulating Solids," in Luminescence of Inorganic Solids (P. Goldberg, ed.) Academic Press, New York, 1966, p. 489.
10. A. Brill and W. L. Wanmaker, "Fluorescent Properties of Some Europium-Activated Phosphors." J. Electrochem. Soc. 111(12), 1363 (1964).
11. G. Blasse and A. Brill, "Investigations of Tb⁺³ Activated Phosphors." Philips Res. Repts. 22, 481 (1967).
12. K. Okamoto and Y. Hamakawa, "Bright Green Electroluminescence in Thin Film ZnS:TbF₃, Appl. Phys. Lett. 35(7), 508 (1979).
13. J. A. Cape, R. Ketchpel and L. Hale, "A Possible Model for Thin Film ac Electroluminescent Devices." 1978, Device Research Conf., Santa Barbara, CA.



14. L. G. Hale, J. Cape and W. F. Hall, "A Model for thin Film ac Electroluminescent Devices," 81st Annual Meeting of the American Ceramics Society, May, 1979.
15. W. Busse et al, "Time Resolved Spectroscopy of ZnS:Mn by Dye Laser Technique." J. Lumin. 12/13, 693 (1976).
16. Y. S. Chen and D. C. Krupka, "Limitation Imposed by Field Clamping on the Efficiency of High Field Electroluminescence in Thin Films." J. Appl. Phys. 43(10), Oct. 1972.
17. R. Shrader, S. Larach and P. Yocom, "Cathodoluminescence Efficiency of Tm^{+3} in Zinc Sulfide." J. Appl. Phys. 42(11), 4529 (1971).
18. J. Benoit, P. Benalloul and B. Blanzat, "Rare-Earth Complex Dopants in ac Thin Film Electroluminescent Cells." J. Lumin. 23, 175 (1981).

DATE
FILMED

2-8